

Design and Analysis of a Water Channel for Characterization of Low Reynolds Number Flows

Judah D. Rutledge, Jesse J. French*

Department of Mechanical Engineering, LeTourneau University, Longview, Texas, USA.

Received 21 July 2017; received in revised form 05 September 2017; accepted 13 December 2017

Abstract

A water channel for performing flow visualization and studying scale models in fluid mechanics was designed, analyzed, and fabricated with commercially available components. The material cost of the channel is 10% of the leading educational units, and the fabrication processes required for channel construction are basic and typical of local craftsmen in developing countries.

Both structural analysis and flow rate calculations were performed to verify the functionality of the tunnel. Hand calculations and finite element analysis were used to model stress and deflection in the channel floor under hydrostatic loads. These were used to select a polycarbonate panel thickness that will withstand the hydrostatic and hydrodynamic loads on the channel floor and walls for a projected useful lifespan of 40 years.

The water channel has a test section area that is 30 cm by 42 cm and up to 1 m long. The system pump is capable of generating incident flows of up to 7.1 cm/sec in the test section. The channel is also designed to be upgraded with a tow carriage, allowing for flow visualization as well as fully submerged and partially submerged models with Reynolds or Froudes number dependent studies.

Keywords: fluid mechanics, aerodynamics, water tunnel, laminar flow, scale model, education

1. Introduction

In order to perform scale model tests that can be correlated with the behavior of prototypes in a real world environment, engineers make use of controlled environments to simulate or duplicate the conditions experienced by a component in operation. Since in-situ testing can often be prohibitive in terms of both cost and time, significant time and attention are given to the scale model testing of prototype. Additionally, scale models can be used to test and observe phenomena that are unmanageable or that happen at rates humans cannot typically observe in real time, be it a phenomenon that occurs in fractions of a second, such as vortices traveling down the length of a swept wing, or that takes months to develop, as in erosion case studies [1]. Finally, scale models are invaluable for gaining deeper understanding of the physical phenomenon being explored. This application, in particular, is invaluable for higher education institutions.

For products finding application in the realm of fluid mechanics, wind and water tunnels are the primary means for achieving the repeatability and control required for such tests. Water tunnels, specifically, are used when testing phenomena related to marine or aquatic applications; they are also used in aerodynamics when detailed flow visualization is necessary. There are several companies that have designed excellent water tunnels for research and education [2]. However, these water tunnels can be expensive and difficult to acquire in developing nations. Because of this, a water tunnel was designed using commercially available components with the end goal of manufacturing an adequate but affordable solution for studying fluid mechanics. Such a tunnel design is affordable, can offer opportunities to smaller institutions in first world countries and to

* Corresponding author. E-mail address: JesseFrench@letu.edu

institutions in developing countries worldwide, and benefits the local economy in the country of construction. This paper describes the economic considerations, the construction of this device, and the structural and flow analysis for the design.

2. Manufacturing and Cost

A CAD model highlighting standard water channel components of the channel assembly is shown in Fig. 1 [3]. The channel structure is constructed in two separate components, both of which are welded out of A36 steel and powder-coated for corrosion resistance. The first component is the channel frame. The frame is constructed out of angle iron in the corners and reinforced with square tubing every 40 cm along the length of the channel to support the sidewalls and to mitigate deformation of the tunnel. These supports also serve to attach fixtures to the channel for model specific tests, for mounting photography equipment, or for attaching rails for a towing carriage or for wave generation. The second component is the work bench. The work bench provides a stable work place for tests and supports the channel tank, which weighs 370 kilograms when filled to capacity. The bench has four adjustable feet which allow for accurate levelling of the channel assembly. The channel itself is 2.4 meters long with a test section that is 100 cm long and a 30 cm x 40 cm. cross-section. The rectangular channel design simplifies construction, though some flow conditioning is lost without a contraction.

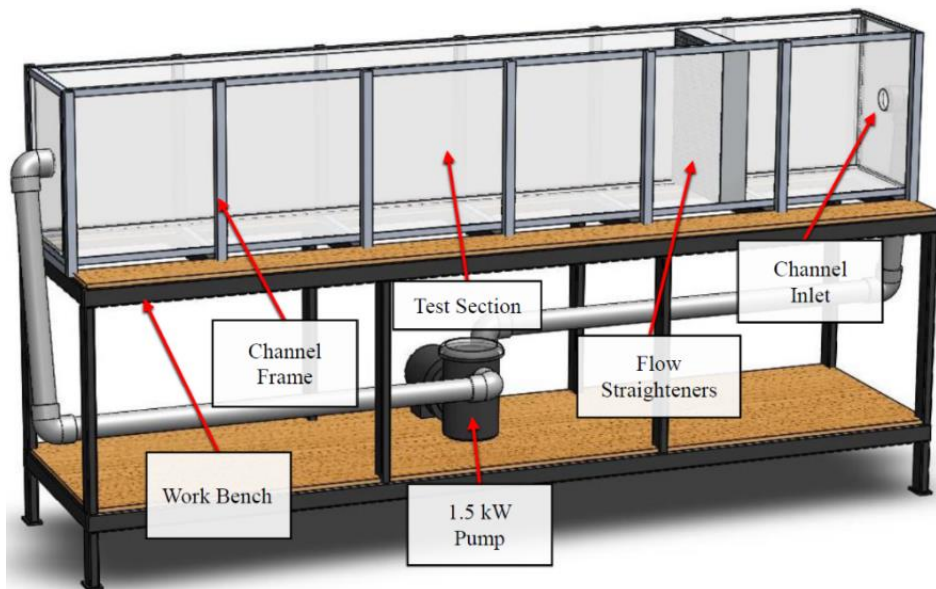


Fig. 1 CAD Model of the water channel assembly

Only materials and manufacturing methods commonly available in developing nations were used for constructing the channel. The work bench and frame were constructed with A36 rectangular steel tubing and powder coated to mitigate corrosion due to contact with water, though the appropriate primer and paint coat would also be adequate. The channel walls and floor were constructed from polycarbonate panels. The bench and frame were welded using gas metal arc welding, though the thickness of steel used can also be stick-welded or oxy-fuel welded if other forms of arc welding are not available. In order to resist distortion and leaking, the enclosure was bonded with SciGrip 16, and sealed along the inner seams with a MasterSeal NP1, a polyurethane sealant rated for continuous water immersion. The channel was plumbed with standard PVC pipes and fittings, and a centrifugal pump was sourced to power the flow loop. The total construction time of the channel from was 2.5 months. Fig. 2 shows the finished channel with the flow conditioners in place.

A cost analysis shows that the channel is highly affordable when compared to the typical cost of an educational water tunnel, which is in the \$20,000 range. Because labor for the construction was a portion of this project, only the material purchases are used to determine the baseline cost of producing a channel unit. The breakdown of material costs is shown in Table 1. The total cost of producing the water channel is 1609.09 USD, which is roughly 10% of the cost for purchasing a commercially produced tunnel for education and research [4].



Fig. 2 Completed Water Channel assembly

Table 1 Material Purchase Costs for the Water Channel

Component	Unit	Cost	Qty	Component Cost
.375x48x96" Lexan	Sheet	567.00	1	417.00
.375x24x48	Sheet	178.21	1	137.24
MasterSeal NP1	Tube	5.36	3	16.08
SCIGRIP 16	Can	12.51	1	12.51
Teflon Tape	Roll	1.48	1	1.48
Silicone Gasket	Unit	2.4	2	4.80
2 in x 10 ft PVC pipe	Unit	8.37	2	16.74
2 in Socket Female x NPT Male	Unit	1.17	2	2.34
2 in Socket Femal x NPT Female	Unit	1.2	2	2.40
2 in 90 Deg Elbow	Unit	0.98	6	5.88
PVC Primer & Cement	Pack	8.81	1	8.81
2 in Threaded Adaptor	Unit	1.32	2	2.64
PVC Primer & Cement	Pack	8.81	1	8.81
Garboard Drain Plug	Unit	10.17	1	10.17
Rubber Gasket	Unit	12.91	2	25.82
Pentair 011515 Whisper Flow	Unit	664.75	1	664.75
Wiring Cable	Feet	2.32	15	34.80
Wiring Plug	Unit	19.97	1	19.97
Double Pole toggle Switch	Unit	5.98	1	5.98
Switch Junction Box	Unit	5.95	1	5.95
8x32 Stainless Steel Screws	Bag/24	6.48	1	6.48
3/8 inch Bolt	Unit	1.61	4	6.44
1"x2"x14 gauge Steel Tubing	24' stick	31.00	3	93.00
.75"x.75"x11 gauge Steel Angle	24' stick	18.00	2	36.00
1"x1"x14 gauge Steel Tubing	20' stick	21.00	3	63.00
Total Cost				1609.09

3. Structural Analysis

Both hand calculations and finite element analysis (FEA) were used for the structural analysis of the channel. Aspects of the channel that were analyzed for failure include critical components such as the table legs, the channel ribs, and the enclosure. Material selection was performed based primarily on availability and cost, and mathematical analyses were performed to determine if the selection was adequate. In order to guarantee that the tank geometry was not compromised, stress and distortion calculations were performed on the frame, the channel walls, the channel floor, and the work bench.

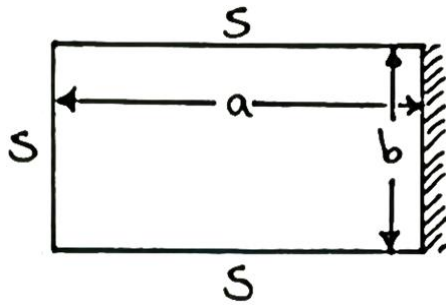


Fig. 3 Plate boundary conditions for floor and ends of channel

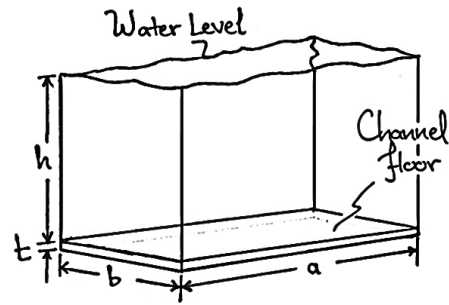


Fig. 4 Hydrostatic pressure on water channel panel

In most of the channel design, the limiting factor was not structural integrity, but was instead deflection. Even if the maximum stresses in a test fixture are relatively small, deflections in the structure can be sufficiently large to affect the geometry of the test section and introduce error in the test data. A secondary concern with deflection is the visual detection by the operator. Visible deflection can detract attention from the test and reflect poorly on the quality of construction of the testing device. Because of the magnitude of the deflections caused by the hydrostatic loads in the channel, visual deflection was the most prominent concern for all of the items evaluated. The maximum deflection allowed for any channel component was 0.1 inches (2.5 mm), which is detectable with measurement devices but is not a misalignment typically visible upon simple observation. The stress and deflection calculations for the floor channel are presented here as a case study of the methods used.

In order to choose the thickness of polycarbonate used for the channel floor and size, the floor panel between two support beams was modeled as a rectangular plate for maximum stress and maximum deflection calculations. Both hand calculations were performed using *Roark's Formulas for Stress and Strain* [5], and various FEA models were created using COMSOL Multiphysics 5.1. Based on the frame geometry, the plate length and width for one section of the channel are 16 inches and 12 inches respectively. Thicknesses of 1/4, 3/8, and 1/2 inch were considered for deflection and stress. Since the channel walls were originally only going to be sealed, not bonded to the floor, they were not considered fixed to the floor, resulting in these sides being simply supported. Where the panel is supported by a frame rib is considered fixed since the loading opposite of the span is nearly symmetrical. These boundary conditions, then, represent the most severe loading condition, that which is at the ends of the channel where three sides of the plate are simply supported, and only the side that is supported by a span of the tunnel is assumed to be cantilevered (Fig. 3).

For the hand calculations, Table 11.4.3 was referred to in *Roark's Formulas for Stress and Strain*. This describes the maximum stress and maximum deflection as a function of plate geometry, the material properties, and an applied, constant pressure. Because the maximum deflection and stress in plates with straight boundaries are determined numerically, no expression for deflection and stress as a function of position is derived. Instead, the dimensionless ratio, a/b is used to characterize plates through a range of aspect ratios and derive empirical constants used in conjunction with the plate thickness and material properties to estimate maximum stress and deflection according to Eqs. 4.1 and 4.2.

$$\sigma_{max} = \frac{\beta qb^2}{t^2} \quad (1)$$

$$y_{max} = \frac{-\alpha qb^4}{Et^3} \quad (2)$$

Here q is a constant hydrostatic pressure equal to the depth of the water times its specific gravity (Fig. 4), E is Young's Modulus, and b and t are the width and thickness of the plate, respectively. The final variables in these equations, β and α , are functions of the aspect ratio, a/b , and are determined by interpolating values from Table 11.4.3 in *Roark's*. The provided tables are for a Poisson's ratio of 0.3. According to the handbook, the returned deflection will be accurate to within 8%, and the maximum calculated stress to within 15% [5].

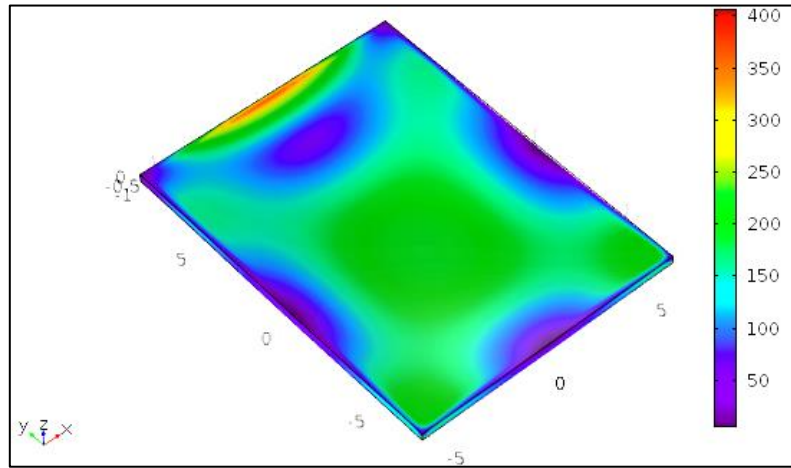


Fig. 5 FEA results for stress distribution on for the channel floor (psi)

The same boundary conditions and geometry were used for the FEA analysis using COMSOL. Since Roark’s analysis is based on a Poisson’s ratio of 0.30, and the actual Poisson’s ratio for polycarbonate is 0.37, FEA models were run for both Poisson’s ratios of 0.3 and 0.37 in order to compare the effects of Poisson’s ratio on the stress and deflection and determine if Roark’s can still be used as an accurate approximation (Fig. 5).

The hand calculations and the FEA models showed a lower correlation for the maximum displacement (Table 2), but high correlation for the maximum stress (Table 3). The maximum error between Roark’s and COMSOL for a Poisson’s ratio of 0.30 was 3% for stress and 18% for displacement. Modifying Poisson’s ratio did not significantly affect the stress or displacement, changing the stress and displacement values by about 1% and 5% respectively. Based on this, the tables in Roark’s handbook for stress and strain of rectangular plates can be used for similar designs where an FEA package is not available. The most important result from this analysis, however, is that the displacement of both the 3/8 inch and the 1/2 inch panel is within the allowable limit of 2.5 mm. Since the 3/8 panel fulfilled the strength and deflection requirements, and the cost difference between the 3/8 inch and the 1/2 inch panels was significant, the 3/8 inch panel was selected for the channel enclosure.

Table 2 Maximum deflection for channel floor [mm]

	Roark’s	COMSOL (nu = 0.30)	COMSOL (nu = 0.37)	Percent Difference [%]	
				CM vs. R (nu=0.30)	nu=0.30 vs. nu=0.37
1/4 inch	3.83	4.47	4.24	14.3	5.4
3/8 inch	1.13	1.34	1.27	15.7	5.5
1/2 inch	0.47	0.572	0.542	17.8	5.5

Table 3 Maximum stress for the channel floor [kPa]

	Roark’s	COMSOL (nu = 0.30)	COMSOL (nu = 0.37)	Percent Difference [%]	
				CM vs. R (nu=0.30)	nu=0.30 vs. nu=0.37
1/4 inch	5615	5587	5559	0.5	0.5
3/8 inch	2495	2424	2450	2.9	1.1
1/2 inch	1413	1401	1414	0.9	0.9

Because the prolonged loading nature of a hydrostatic pressure vessel makes such structures susceptible to creep when constructed from polymers, a creep rupture stress analysis was also performed on the panel [6]. A literature review for the creep rupture properties of polycarbonate showed that available plots only predicted the creep rupture strength out to 45,000 hours, or approximately 5 years [7]. However, since the creep rupture stress curve for polycarbonate showed a highly linear trend on a logarithmic scale, an extrapolation out to one more order of magnitude was also performed. These estimations predicted that the panel has a very high factor of safety with respect to creep rupture over the channel’s design life. The creep rupture strength at five years is 49,000 kPa, and the estimated the rupture strength decreases to 43,000 kPa at 40 years of continuous loading. Still, the panel stress at 40 years is only 6% of the estimated rupture strength for this loading period. This estimation produces a factor of safety of 16.7, indicating that the channel floor and walls are not at risk of failing due to creep.

4. Flow Rate Analysis

When determining the channel flow rate, two systems were considered: a pump providing constant flow rate and a surge tank which could potentially provide higher flow rates for a short period of time. The flow rate calculations for both systems were performed based on the dynamic head source and pipe and fitting friction factors determined from the literature. Because the pump and hardware used were specified in English units, all head and flow rate calculations were performed in the same, and the final flow velocity in the channel test section was then converted into centimeters per second.

4.1. Surge tank flowrate

The surge tank flow rate calculations were performed for a surge tank located nominally 10 feet (3 m) above the pipe entering the channel. This head was assumed to be constant, regardless of the level of water in the 200 liter drum chosen as the surge tank. In order to calculate flow rate, an energy balance was performed between the barrel outlet and the channel inlet using the dynamic head, elevation change, and frictional loss coefficients for each component in the system (Eq. 3). Here, P/γ is the dynamic head, l and D are the length and diameter of the pipe, and f and K_L are frictional loss coefficients (Fig. 6). The loss coefficients for pipe fittings, $\sum K_L$, are Reynolds number independent and obtained from tables in *Fundamentals of Fluid Mechanics* by Munson, et. al. [8]. The loss coefficient in the pipe, f , is Reynolds number dependent and was determined using the method outlined by Lewis. F. Moody for pipe flow friction factors [9]. As recommended by Munson, et. al., the pipe was assumed to be smooth, therefore the ratio of the equivalent roughness pipe diameter, ϵ/D , was equal to zero.

$$\frac{P_1}{\gamma} + \frac{V_1^2}{2g} + z_1 = \frac{P_2}{\gamma} + \frac{V_2^2}{2g} + z_2 + f \frac{l}{D} \frac{V^2}{2g} + \frac{\sum K_L V^2}{2g} \tag{3}$$

Velocity at the entrance and exit of the pipe is constant, and the equation simplifies to:

$$z_1 = f \frac{l}{D} \frac{V^2}{2g} + \frac{\sum K_L V^2}{2g} \tag{4}$$

From this, the velocity of the water in the pipe can be solved for as:

$$V_p = \sqrt{\frac{z_1 2g}{f \frac{l}{D} + 2K_L}} \tag{5}$$

Fig. 7 shows the iterative process used for calculating water velocity in the channel pipe. First, a frictional loss coefficient, $f(Re)$, is assumed. From this, the velocity in the pipe is calculated using Eq. 5, and the flow Reynolds number is calculated for this velocity and pipe diameter:

$$Re(V_p) = \frac{\rho DV}{\mu} \tag{6}$$

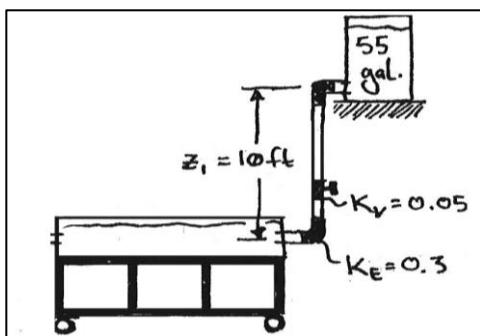


Fig. 6 Surge Tank geometry and loss coefficients

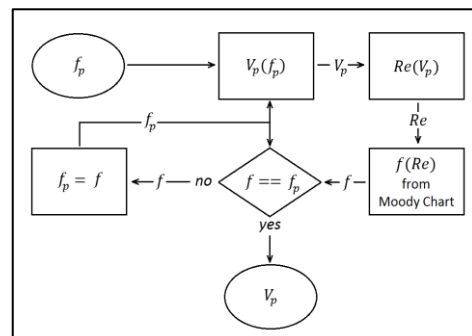


Fig. 7 Logic diagram for determining velocity from constant head

By referring to a Moody flow chart, this Reynolds number is then used to determine a new frictional loss coefficient. This process is repeated until the loss coefficient converges to a value. The last calculated velocity is then the velocity in the pipe and is used to determine the flowrate in the water channel. Using this approach, the pipe flow velocity was determined to be 233 in/s in the channel pipes, which corresponds to a speed of 8.3 cm per second in the water tunnel.

4.2. Pump Flowrate

The Pentair WhisperFlo 011515, rated at 1.5 kW of power, was selected as the second candidate for running the water channel. The flow rate generated by the pump in the water tunnel is calculated with a procedure similar to that used for the surge tank calculations, the primary difference being that a pump does not provide a constant head. Therefore, the pump head, $H(Q)$, had to be incorporated into the iterative solution for channel flow. The dynamic head generated by a pump is dependent on flow rate, which introduces another step in the iterative process used to determine the speed of the water channel. Since a dynamic head, P_1/γ , is present because of the pump, but there is no net change in elevation by the water across the flow loop (Fig. 8), Eq. 3 takes on the form:

$$H = \frac{P_1}{\gamma} = f \frac{l}{D} \frac{V^2}{2g} + \frac{\sum K_L V^2}{2g} \tag{7}$$

In order to determine the flow rate generated by the WhisperFlo 011515, the dynamic head was assumed to be equal to the head drop across the piping of the water tunnel, and the pressures at the entrance and exit of the channel were assumed to be equal to atmospheric pressure. Because flow rate, head, and viscous friction are interrelated, an iterative solving approach was once again implemented (Fig. 9), where the flow rate was determined from the pump performance curve for the WhisperFlo 011515 (Fig. 10). In order to solve for the flowrate, a dynamic head of 20 ft was assumed, and the flowrate was determined from the pump performance curve. The pipe friction factor was calculated from the Moody chart for this Reynolds number, and the actual head was calculated from V_p and f . Flow rate was determined for this new calculated head, and the process was iterated until the calculated head converged to 10.9 ft of water. From this head, the velocity in the pipes was determined to be 208 in/s, and the calculated speed in the water channel was 7.4 cm/s.

According to these calculations, the surge tank and the WhisperFlo generate water speeds in the channel that vary by only 0.9 cm/second. Therefore, there is no significant advantage to constructing a surge tank for attaining greater flow rates. Additionally, implementing a surge tank requires the design, construction, and space allocation of a tower to support the water, and a surge tank will not generate a truly steady flow, since the level in the surge tank changes the actual head by 40% as it drains. Finally, this design would not be capable of continuous operation, would require significant modification to change the functionality from a flow channel to a tow channel and would still require the purchase of a pump to move water from the bottom reservoir up to the surge tank. Since all of these factors are resolved by using a pump to continuously power the system, and the flow rate gain from using a surge tank is negligible, a pump was selected as the head source for generating flow in the water channel. These calculations were validated after the channel was completed. The flow velocity distribution had a maximum speed of 7.1 cm/second in the center and 5.6 cm/second near the walls within the boundary layer.

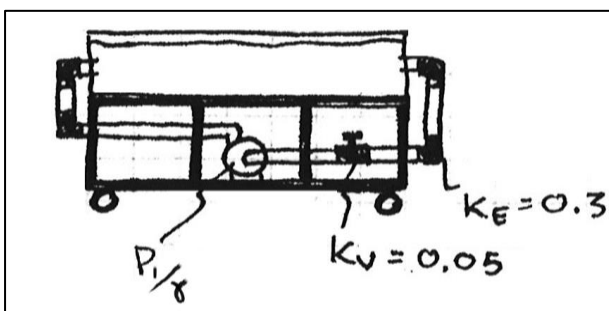


Fig. 8 Channel pump head and loss coefficients

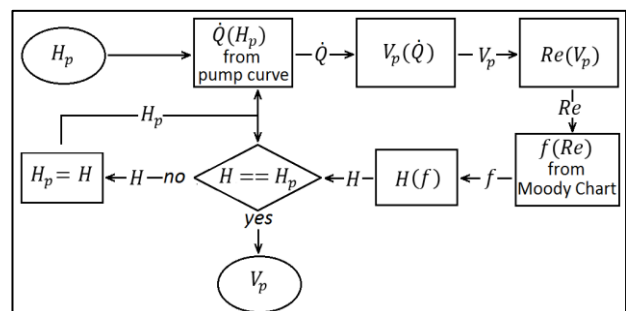


Fig. 9 Logic diagram to calculate velocity generated by pump

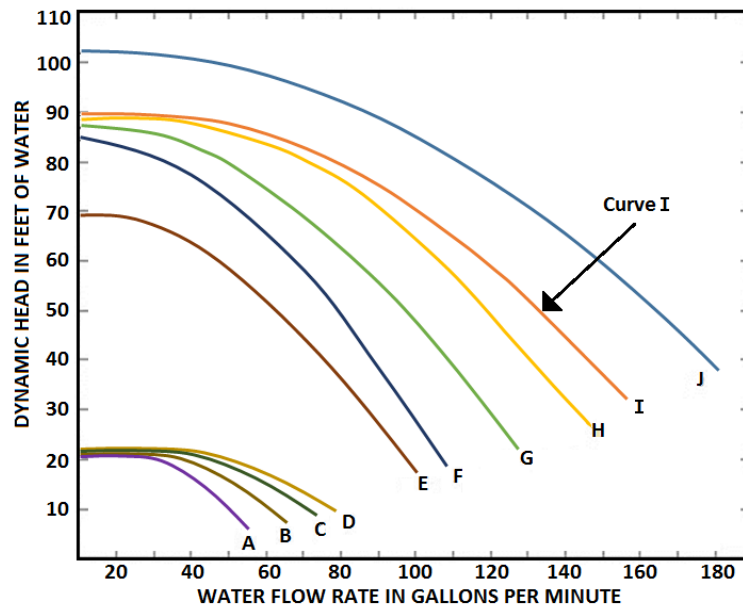


Fig. 10 Performance curve for the Pentair WhisperFlo line of pool pumps. Curve I corresponds to the model 011515 [10]

5. Conclusions

A water channel for flow visualization and scale model testing was successfully designed and manufactured using components and manufacturing methods that are globally available. Structural analysis and flow rate calculations were used to predict tunnel performance based on available materials. A high correlation was found between FEA models and the hand calculations using standard texts. Flow estimations using pipe flow and pipe fitting friction factors were used to predict the dynamic head source for the water channel. Maximum flow rate calculations correlated closely to measured velocities in the test section.

The frame and work bench are welded from mild steel, and the channel test section is constructed from clear polycarbonate. The channel workbench footprint is one meter wide and 2.4 meters long, and the test section is 100 cm long with a 30 cm x 40 cross-section. The total cost of materials for manufacturing the channel was 1 609.09 USD. This water channel provides an economic alternative for education or basic research of low Reynolds number flows.

References

- [1] R. I. Emori and D. J. Schuring, *Scale models in engineering: fundamentals and applications*, Great Britain: A. Wheaton & Co. Ltd., 1977.
- [2] Rolling Hills Research, "Water Tunnel Model 0710," www.rollinghillsresearch.com/Water_Tunnels/Model_0710.html
- [3] Engineering Laboratory Design, Inc., "Water Tunnels," <http://www.eldinc.com/pages/0246;WATERTUNNELS/>
- [4] Y. Farsiani and B. R. Elbing "Characterization of the custom-designed, high reynolds number water tunnel," Proc. Of the ASME Fluids Engineering Division Meeting, 2016.
- [5] W. C. Young and R. G. Budynas, *Flat plates*, 7th ed. New York: McGraw Hill, 2002.
- [6] J. Jansen, "Understanding creep failure of plastics," *Plastics Engineering*, Society of Plastics Engineers, 2015.
- [7] P. J. Gramann, J. Cruz, and J. A. Jansen, "Lifetime prediction of plastic parts," Proc. in Annual Technical Conference, 2012, pp. 1313-1318.
- [8] B. R. Munson, D. F. Young, and T. H. Okiishi, "Fundamentals of Fluid Mechanics - dimensional analysis of pipe flow," 6th ed. New Jersey: John Wiley & Sons, inc., 2002.
- [9] L. F. Moody, "Friction factors for pipe flow," *Transactions of the American Society of Mechanical Engineers*, pp. 671-682, 1944
- [10] WHISPERFLO High Performance Pump, "Whisperflo curves," <http://www.pentairpool.com/products/index.html>.